Article citation info:
Tytuła J, Zaremba A, Nitkiewicz S. Evaluation of forces in a racing simulator based on a Stewart platform. Diagnostyka. 2023;24(4):2023405. https://doi.org/10.29354/diag/171729.

DIAGNOSTYKA, 2023, Vol. 24, No. 4

e-ISSN 2449-5220
DOI: 10.29354/diag/171729

EVALUATION OF FORCES IN A RACING SIMULATOR BASED ON A STEWART PLATFORM

Jakub TYTUŁA [1], Arnold ZAREMBA [1], Szymon NITKIEWICZ [1, 2 *],

[1] Department of Mechatronics, Faculty of Technical Sciences, University of Warmia and Mazury, 11 Oczapowskiego St., 10-710 Olsztyn, Poland,
[2] Department of Neurosurgery, School of Medicine, Collegium Medicum, University of Warmia and Mazury, 30 Warszawska St., 10-082 Olsztyn, Poland
[*] Corresponding author, e-mail: szymon.nitkiewicz@uwm.edu.pl

Abstract

This paper presents how forces are perceived in a racing simulator based on a Stewart Platform. By retrieving calculated forces in a racing game by its physics engine and comparing them to real-life measurements during the platforms motions it is possible to evaluate the platforms immersiveness. Virtual values extracted from the game engine are deemed satisfactory to their real life counterparts and serve as a baseline. In order to evaluate forces created by the simulator, a lap around a virtual test track is recorded and played back while an accelerometer and gyroscope record its movements. Overall, accelerations recorded in the direction of X and Y axis along with angular speed of rotation around the aforementioned those axis. To accurately comparing every derived force, the recorded virtual lap is divided into sections representing the five most common manoeuvres during racing. These comparisons serve as an evaluation method to measure the immersiveness of the simulator.

Keywords: Stewart platform, force, race simulator

1. INTRODUCTION

Every force which is felt by the driver of a car feels is caused by their own inertia. While driving a car on a race track, during long straights, not much driver input is needed, and not much force is felt by the driver. Only acceleration and deceleration are felt by their longitudinal forces. This force during acceleration is dictated by the power curve of the car's engine [1-5]. This force pushes the driver into his seat. The maximum g-force is reached when the maximum torque is transferred to the car wheels, whether this torque is derived from breaking or accelerating. When shifting gears the sudden lack of torque and consequently the sudden lack of g-force is felt by the driver. Under braking g-force tends to force the driver into their seatbelt. While cornering, if a vehicle turns to one side, the driver experiences a force that pulls them in the opposite direction. Figure 1 shows the direction of inertia during cornering. These forces and many others are what need to be simulated in a motion platform.

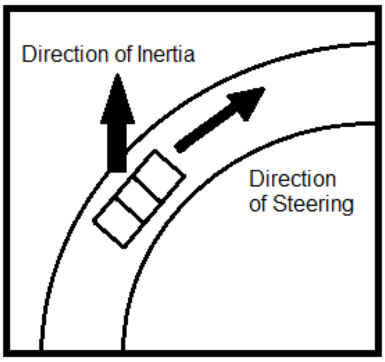

Fig. 1. Direction of inertia during cornering

The motion simulator presented in this paper is based on a Stewart platform. Figure 2 shows the motion platform. It features six linear actuators powered by brushed DC motors driving a trapezoidal lead screw, which, in turn, translates rotary motion into linear motion. There are six actuators in total, divided into three pairs. These pairs form triangular-shaped mounting points on its baseplate and cross over to three other mounting points located on the simulators top plate which acts as a cockpit. Universal joints made from universal car steering joints make up the attachment points. Due to this arrangement the cockpit is able to move within six degrees of freedom. This allows for three linear movements and three rotations. The range of motion is mainly limited by the platform mounting points radius and the stroke of the linear actuators. The

Received 2023-08-09; Accepted 2023-09-01; Available online 2023-11-03

maximum acceleration is limited by the speed of its motors.

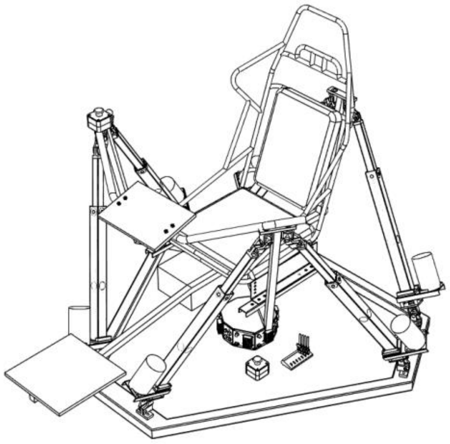

Fig. 2. Motion platform

The motion simulator presented in this paper is based on a Stewart platform. Figure 2 shows the motion platform. It features six linear actuators powered by brushed DC motors driving a trapezoidal lead screw, which, in turn, translates rotary motion into linear motion. There are six actuators in total, divided into three pairs. These pairs form triangular-shaped mounting points on its baseplate and cross over to three other mounting points located on the simulators top plate which acts as a cockpit. Universal joints made from universal car steering joints make up the attachment points. Due to this arrangement the cockpit is able to move within six degrees of freedom. This allows for three linear movements and three rotations. The range of motion is mainly limited by the platform mounting points radius and the stroke of the linear actuators. The maximum acceleration is limited by the speed of its motors.

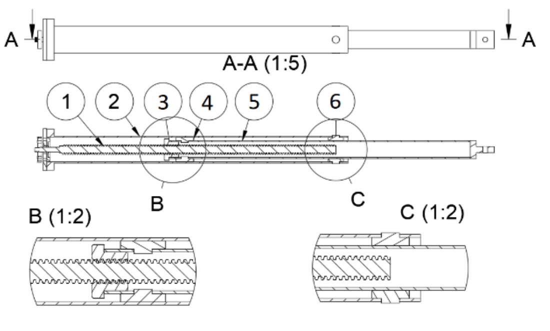

Fig. 3. Detailed view of an actuator

Figure 3 shows a detailed view of a single actuator. Cross-section view (A) shows the inner workings of an actuator. It can be divided into three main sections: the actuators housing (2), inner piston (5) and leadscrew (1). The housing serves two purposes, it acts as the lower mounting point for its universal joint and as an outer slide and guide for its piston. In its upper section, which can be viewed in closeup (C), it has a total of four holes for mounting slide bushings (6). These slide bushings are what the piston rides on and restricts its rotational movement due to the fact that both the housing and the piston are made from square tubing. The lower part that has a mounting point for the lower universal joint also contains two bearings. One roller bearing and one thrust bearing both for the leadscrew. A motor mounting bracket is also sandwiched between the universal joint and the actuator housing. The inner piston is restricted to linear motion due to the aforementioned square tube design and slide bearings (4). It also has four holes into which four slide bearings fit located in its lower section. These bearings ride on the inner section of the actuator housing. Also in its lower section there is a screw driver nut (3) pressed in and secured by screws which is shown in view (B). The leadscrew nut is made from bearing bronze. The upper part of the inner piston has a mounting point for the upper universal joint. The leadscrew itself is made of one piece. It is a TR16x4 rod with features machined into one of its ends. These features include press-fit bearing surfaces and a keyway with a locknut for belt driven pulley. This belt drive provides rotational motion to the leadscrew which in turn slides the inner piston in and out of its housing.

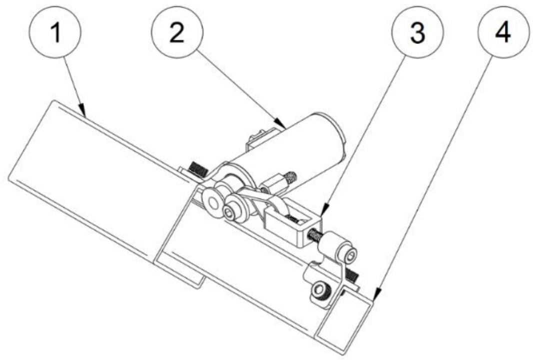

Fig. 4. View of the feedback components

In order to give feedback of the piston position to the software a self-made hall effect potentiometer is used. Figure 4 shows a view of the feedback loop components. This feedback loop can be divided into two sections: the hall effect potentiometer (2) and a belt tensioning mechanism (3). The hall-effect potentiometer is mounted to the upper section of the actuator housing. The belt tensioner is mounted on the upper part of the inner slide. The belt itself is fixed on one end by looping around a mounting point on the inner slide and by looping around a 3D printed bracket on the other side. Both ends are then secured with zip ties meshing the belts teeth. In order to maintain proper teeth engagement with the potentiometer leadscrew pulley an offset idler pulley is added. The belt tension is adjusted with a screw going through the 3D printed bracket which holds one end of the belt. The main benefit of using a hall-effect potentiometer instead of a regular mechanical potentiometer is durability. Contactless detection of dynamic input greatly increases service intervals. During the initial testing of a prototype motion platform, multi-turn potentiometers were used. Unfortunately, after prolonged use their contact points inside their housing wore down in certain areas and made them unusable. The only part that wears down with time is the inner pin and nut assembly. Even then, this is a far more durable and cost-effective solution than a regular potentiometer.

The potentiometer itself consists of eight elements, which are shown in Figure 5. Two bearing housings and bearings for the leadscrew (1). The outer shell (2) with its mounting bracket (4). The hall effect sensor (3). A timing belt pulley (5) which is fixed to the leadscrew (8). The lead screwdriver with its magnet (7). The inner hexagonal slide (6). The inner workings of the hall effect feedback potentiometer are shown in the cross-sectional view (A). The hall-effect sensor sits inside the potentiometer housing. While the inner slide moves with its belt attached, it forces the potentiometers pulley to rotate. When the pulley which is affixed to the lead screw turns, it forces a nut with a permanent magnet glued to it to move linearly. A hexagonal slide restricts the rotational movement. This linear motion of the magnet is picked up by the hall sensor which interprets this varying magnetic force into a readable signal. One or two magnet-equipped nuts can be used if one magnet does not have enough force. If two are used, they must be faced with opposite poles to each other. This multiplies their magnetic force, allowing for longer linear motion and finer detail.

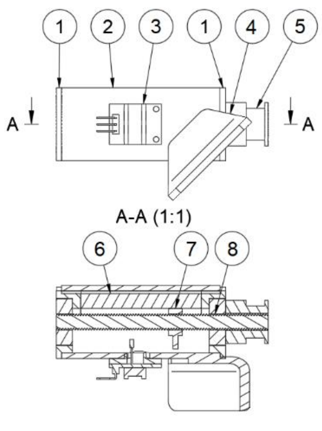

Fig. 5. Detailed view of hall effect potentiometer

In order to evaluate the motion platforms immersiveness, two factors are brought into consideration. Its ability to recreate g-forces that occur during racing in real life and what the user feel when driving in a virtual race. This virtual race is created within Live For Speed, published by Scawen Roberts and Eric Bailey. This racing game accurately simulates forces directly on each wheel of a virtual car. This allows for a very fine and precise feeling on what is happening between the contact patch of a tyre and the road. Moreover, the physics engine calculates tyre wear, suspension, aerodynamics, clutch wear and car body and engine damage. Figure 6 shows how complex the tyre model is. Just this tyre simulation model allows for dynamic thread wear, traction affected by temperature, and sidewall deformation. This racing simulator has been proven more than once to be incredibly accurate and is suited more than enough for this experiment.

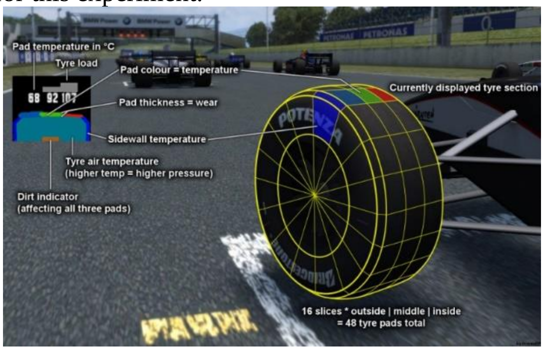

Fig. 6. LFS tyre model [6]

A baseline must be used for comparison against the movements of the motion platforms. This baseline is a lap of the virtual racetrack Blackwood GP. A lap is recorded containing turns, a chicane, a long straight and a head-on collision. This set of manoeuvres represents most of the movements enacted during the race. Consequently, for ease of comparison, specific manoeuvres are compared to each other. FlyPT which is used as an interface for retrieving information from games and using that to move a motion platform. It also allows to record this information gathered from a lap and play it back at any given moment. A graphic viewer enables a visual representation of forces achieved during a lap. This is used to extract individual movements for further comparison.

The FlyPT mover made by Pedro Antunes is used for interfacing LFS with the motion platform electronics. It is a software interface used to convert poses into actuator positions. It extracts game information on the virtual vehicles position, physics, and world geometry. It has a compatible list of games that includes most if not all racing simulating games and even flight or other vehicle simulators. By defining a motion simulator rig with all its measurements, this software can then generate actuator position values. This data can then be sent to any motor driver which operates each actuator motors and provides motion to the platform. In this case, three Arduino Uno's with loaded SMC3 code made by RufusDufus is used. SMC3 uses a PID motor control loop that can provide one Arduino Uno board to control the position of up to three motors using analogue feedback. On this motion platform, three Arduino Uno's control each pair of motors. This is due to hardware limitations of the Arduino Uno board, which cannot provide optimal PWM frequency to three motors at once. Motor drivers from BTS7960 are paired with each DC motor. The workflow of a motion platform connected to a PC running a racing game is as follows. FlyPT mover extracts data from a racing game, in this case LFS. It calculates each actuators position based on the provided measurements of the real motion rig. This constant flow of positional data is sent to three Arduino Uno’s. Each Arduino Uno interprets these data and sends a PWM signal to the motor drivers while reading the position of the actuators from the analogue feedback potentiometers [7].

Phyphox is used to record acceleration and velocity data from the motion platform. It is a smartphone app that makes use of the internal gyroscope and accelerometer, in this case a BOSCH BMI260 unit. It allows for 16-bit accuracy of both its components. The smartphone is placed in the upper platform within the cockpit, which is shown in Figure 7.

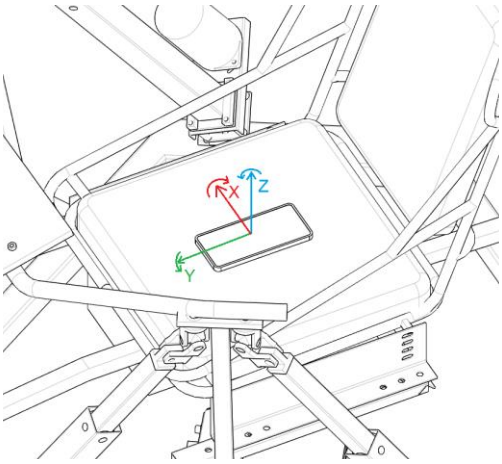

Fig. 7. Smartphone position during testing

This is determined to be a suitable placement for a recording device due to its ease of access and it also coincides with the center of gravity of the upper platform. Data is then recorded and captured into a CSV file that can be read by FlyPT. FlyPT then has an option to filter and condition input signals. An EMALP filter is used for each signal. It is a sample based filter where previous input values are used. Its abbreviation stands for exponential moving average low pass [2, 5, 8]. The EMA portion of the filter is a way to calculate an average value. It uses the same methodology as a regular average by adding values and the dividing the sum of those vales by the amount of added values and also uses a weight system, where older values have lower weight than newer values. The weight of these values varies exponentially. This is a fast way to smooth a signal and requires low computing power. The low pass portion of the filter allows low frequencies to pass unfiltered. This provides smooth feedback and feel that translate the majority of the virtual vehicles movement while maintaining small details like road imperfections and slight steering wheel corrections.

2. RESEARCH METHODOLOGY

As detailed before a baseline is needed. Blackwood GP is loaded along with a recreation of a real car, a Formula BMW FB02. Speed and race time is not the main goal, only the accurate portrayal of specific movements. The lap starts by a quick acceleration going through three gears to the first righthand hairpin turn. During this maneuver the accelerator pedal is let go, focusing on the generated lateral forces. Next is a chicane coming in from the left. This is driven at the limit of traction. After that there is a long straight where acceleration and deceleration is tested. Both to and from 100 km/h and 200 km/h. After that a long right hand turn is also driven at the limit of traction and a head on collision at 100 km/h is recorded. This concludes the baseline. This baseline is then conditioned by an EMALP filter in FlyPT and divided into 5 specific maneuvers: acceleration, deceleration, turning, going through a chicane and finally a head on collision. For ease of comparison a visual representation will be compared.

As for the real life simulated movements in the motion platform, the aforementioned baseline is played back in FlyPT using its player source feature. A smartphone is placed on the seat of the rig and Phyphox is used to record the motion platforms movements. It goes through the sequence of motions recorded in the baseline. Next the recorded data is saved into a CSV file which can be read by FlyPT. The signal is also conditioned and screen recordings of the 5 specific maneuvers are saved. The before and after conditioning plots are presented in Figure 8 and Figure 9.

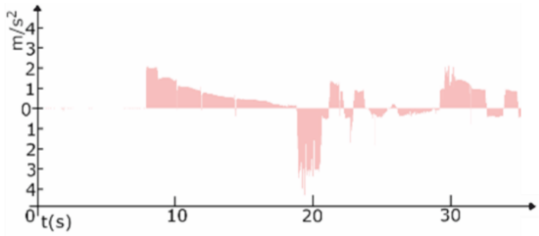

Fig. 8. Sample data before conditioning

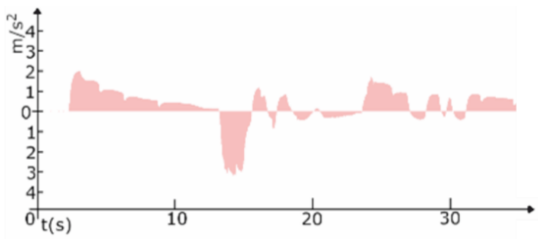

Fig. 9. Sample data after conditioning

After retrieving all the data, value axis are added for ease of interpretation. G-forces and angular velocity are compared. This is due to the fact that a motion simulator with a static base cannot sustain prolonged g-forces. The specific amount of time depends on the maximum force value and the stroke of the actuators. The question is whether or not they are comparable to supposable real life values. Afterall when a person is seated inside the cockpit and is driving a virtual car the immersion level is quite high. This is a subjective statement at the goal of this paper is to somewhat quantify the level of immersion.

3. RESULTS

3.1. Straight line acceleration

When analyzing straight line acceleration only longitudinal forces are taken into consideration. Plots containing this data are in Figure 10. In an ideal pass no lateral forces are present. During this pass the car shifted through four gears. Looking at the baseline recording, during the first gear pull halfway through it there is a noticeable step down. This was caused by wheelspin and subsequent regain of traction. Between each gear shift there is an observable dip. This is due to clutch disengagement and sudden loss of wheel torque during gearshifts. Also a key note, as going up in gears the gear ratio tends to match engine speed and transmission output speed [2, 9-11]. This can be observed as the plot has a downwards tendency due to the consecutive smaller gear advantages reducing torque at the wheels.

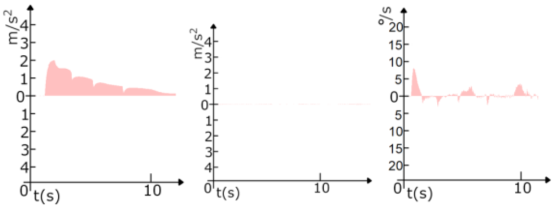

Fig. 10. Recorded longitudinal data with acceleration

Moving on to real life simulated acceleration values it can be seen that there almost is no acceleration. What recorded forces there are, can be considered as noise. Even though a formula BMW car is being simulated, there is not enough linear speed and travel in these actuators to generate conceivable amounts of acceleration. This statement will continue throughout every simulated acceleration plot recorded on the motion platform.

Finally there are angular velocity values. These values are what give the sense of speed and imitate movements of a car in real life. When the gas pedal is pressed the cockpit immediately tilts back at a rapid pace and slowly moves back into its home position coinciding with the baseline acceleration forces. Each gear shift is also recorded and can be viewed on the screengrab. Even slight peaks corelating to the virtual engines torque curve can be noticed. These small details quantify the immersion factor.

3.2. Straight line deceleration

As per the previous acceleration plots, this deceleration will only contain longitudinal forces. This data is in Figure 11. What can be seen on the baseline plot is hard braking while going down gears. Two dips are observed which tell that two downshifts occurred. Downshifting while braking reduces the overall braking distance since it also incorporates engine braking [13-15]. This means that this type of braking has much more perceivable force compared to braking with just the brake pedal. Also because of brake fade, the longitudinal force weakens with time.

Just like the previous real life simulated acceleration, there is almost nothing to note about this plot. There is some more deviation compared to the previous plot, unfortunately even though in comparison to the previous acceleration plot there is more recorded movement, nothing of value can be retrieved and interpreted.

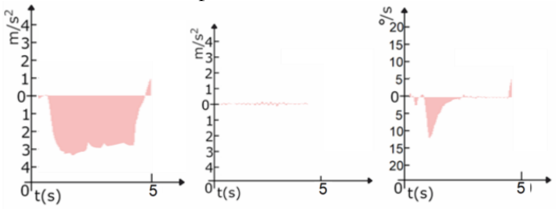

Fig. 11. Recorded longitudinal data with deceleration

Continuing with the angular speed plot it is apparent that it closely resembles the movements within the baseline plot. Rapid and intense forward tilt is held mostly throughout the maneuver. Two slight dips can be noticed where downshifts occurred however they are miniscule. This may be caused by extreme tilt values where definition is lost due to being close to the platforms limits.

3.3. Right hand hairpin turn

While inspecting turning recordings only lateral values are viewed. This turning data is in Figure 12. This is due to the fact that professional drivers while going through a turn maximize their usage of lateral grip for fast cornering, while longitudinal grip is reserved for acceleration and braking [11, 14-16]. On the baseline plot it can be seen that the turn did not go smoothly. There are multiple bumps and dips indicating slight corrections of the steering wheel during the turn. Even as far as turning the steering wheel the opposite way during the turns exit.

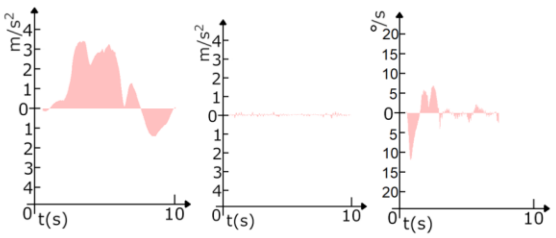

Fig. 12. Recorded turning data

Just as the previous real life acceleration values on the simulator not much can be interpreted from this plot. Slight points of intensified motion can be seen, yet they are negligible. Most likely these small movements would not be recognized by the driver.

When it comes to angular speed values it is a completely different case. These fast and intense movements are almost identically similar to the baseline plot. At least visually. This proves that the algorithm responsible for sending positioning information to the actuators uses tilt values for creating the illusion of g-force. Each sway from side to side while correcting the position of the car is converted into cockpit tilt.

3.4. Chicane

The chicane starts with a righthand entry following the shape of the letter S. The recorded chicane data is presented in Figure 13. In the baseline plot four distinct sections can be observed. Starting with the first turn in. It is rather smooth and precise not having any steering corrections. While the moving through the middle section a slight correction can be seen as well in the last turn. The chicane exit is also smooth with no corrections.

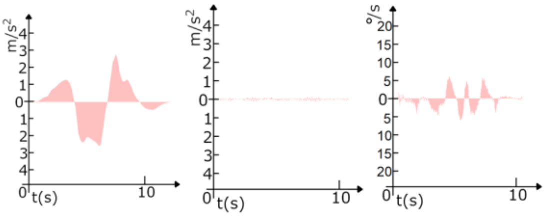

Fig. 13. Recorded chicane data

Due to the smoothness of the maneuver looking at the acceleration plot not much can be seen. Two intensified regions can be distinguished, yet their impact would be small on the driver. This is most likely due to feedback noise rather than intentional acceleration values.

On the other hand the angular speed plot closely resembles the baseline plot. Each movement has its own resemblance in tilt values. Going so far as almost tilting the cockpit to its homing position while correcting the steering wheel during turns. This is most likely caused by the setup of this simulator preferring to exponentiate small movements while maintaining the overall feeling of a maneuver. This once again proves that simulators of this type use gravity to their advantage when trying to simulate acceleration values.

3.5 Head on collision

The head on collision served as a benchmark to test maximum force values of the simulator. The virtual car headed straight on a barrier at approximately 100km/h which resulted in peak longitudinal and lateral force values. This data can be viewed in Figure 14. Due to minor imperfections when hitting the barrier, the vehicle bounced back and spun out. This can be seen on the baseline plots, where after the initial peak force value there are still some movements before the car comes to a complete stop.

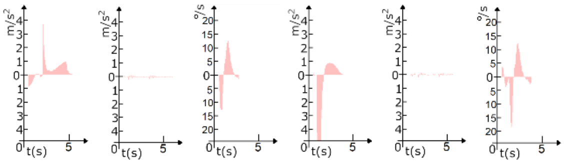

Fig. 14. Recorded collision data

Moving on to the real life acceleration values on the simulator the highest record acceleration values are shown. These are still very minute, yet can be considered as somewhat accurate representations of interpreted acceleration forces. These real life acceleration values on the simulator serve as benchmark of the machine and aim to represent motion platform immersion as not just raw acceleration values. Little details build the whole illusion.

Following with the last set of angular speed plots, once again they closely resemble the baseline plots. These also serve as benchmark and show the maximum speed and tilt achieved during extreme scenarios. Even though such movements put a strain on a motion platform of this size there is still room to simulate small details during such event. This once again shows that racing motion platforms trick the user into feeling the same forces in a real car, since due to their construction even remotely similar acceleration values are impossible to achieve.

4. CONCLUSION

An initial attempt to compare virtual accelerations with real accelerations did not yield the expected results. Sitting in the cockpit and feeling the so far unidentified forces it is safe to say that the immersion is in all respects impressive. However in reality after analyzing the accelerations alone the results say quite the contrary. It is impossible for a stationary simulator with limited actuator stroke to maintain a constant acceleration value. The acceleration value depends on the speed of the actuator, which in turn is determined by its motor speed and its leadscrew thread pitch. The duration of acceleration depends on both actuator stroke and speed. A given high acceleration value will quickly exhaust the range of the actuator and after reaching this maximum stroke extension value, the actual total felt acceleration will be zero. Therefore, the simulator loses its illusion when performing long maneuvers, but not fully. To maintain immersion, the simulator uses gravity. To effectively evaluate the performance of this platform's motion, it is necessary to take into account not only the accelerations themselves, but also its angular velocity [5, 8, 17]. Hence the need to compare the plots of virtual accelerations to the real life simulated angular velocities. Comparing the acceleration values to the angular velocity values, one can conclude that they are visually very similar. This somewhat reveals the control algorithm of the actuators, which tends to mimic acceleration values with angular tilt values. After a deeper analysis of the construction of motion platforms their limits are known and to compensate for acceleration limitations the program uses roll angles to create the illusion of constant force. Therefore, on a long turn there is the impression that the driver is constantly being physically pushed out of the turn by the platform tilting so much that gravity pulls the driver out of his seat. Playing a virtual game and looking at the image displayed by the computer, the driver's mind tricks itself into thinking that he feels centripetal force. In reality once the seat reaches the amount of tilt required in a turn it physically pushes the person off the seat by the driver's mass of inertia. Likewise, when braking or accelerating, the tilting seat either pushes the driver deeper into the seat or pushes him out of it. It is the combination of the imagination of the person behind the wheel of the simulator and the tilt angles that are mainly responsible for the immersion of motion platforms. The more experienced the driver, the less range of motion is required to achieve a satisfactory effect. In fact too much range of motion breaks the illusion as the driver will focus more on the moving platform than the virtual track. In such constructions balance is important to achieve the perfect illusion. All the movements performed are only there to subtly help a person's imagination to complete the real-world forces.

Author contributions: *research concept and design, J.T., S.N.; Collection and/or assembly of data, J.T., A.Z.; Data analysis and interpretation, J.T.; Writing the article, J.T., A.Z., S.N.; Critical revision of the article, S.N.; Final approval of the article, J.T., S.N.*

Declaration of competing interest: *The authors declare that they have no known competing financial interests or personal relationships that could have appeared to influence the work reported in this paper.*

REFERENCES

1. Korf I. You suck at racing: a crash course for the novice driver. CreateSpace Independent Publishing Platform 2016.
2. Kang C-G. Closed-form force sensing of a 6-axis force transducer based on the Stewart platform. Sensors and Actuators A: Physical 2001; 90(1–2): 31–7. https://doi.org/10.1016/S0924-4247(00)00564-1.
3. Zhou S, Sun J, Chen W, Li W, Gao F. Method of designing a six-axis force sensor for stiffness decoupling based on Stewart platform. Measurement 2019;148:106966. https://doi.org/10.1016/j.measurement.2019.106966.
4. Chi W, Ma H, Wang C, Zhao T. Research on control of Stewart platform integrating small attitude maneuver and vibration isolation for high-precision payloads on spacecraft. Aerospace 2021; 8(11): 333. https://doi.org/10.3390/aerospace8110333.
5. Dasgupta B, Mruthyunjaya TS. The Stewart platform manipulator: a review. Mechanism and Machine Theory 2000;35(1):15–40. https://doi.org/10.1016/S0094-114X(99)00006-3.
6. LFS tire model [Internet]. 2008 [cited 2023 Jul 14]. https://manolete.files.wordpress.com/2008/07/explicacion-temp-rueda.jpg.
7. Barański R, Galewski M, Nitkiewicz S. The study of Arduino Uno feasibility for DAQ purposes. Diagnostyka 2019;20(2):33–48. http://dx.doi.org/10.29354/diag/109174.
8. Zhang Y, Han H, Zhang H, Xu Z, Xiong Y, Han K Li Y. Acceleration analysis of 6-RR-RP-RR parallel manipulator with offset hinges by means of a hybrid method. Mechanism anad Machine Theory. 2022; 169: 104661. https://doi.org/10.1016/j.mechmachtheory.2021.104661.
9. Lopez C, Sullivan D. Going faster!: mastering the art of race driving: the skip barber racing school. Bentley Publishers 2003.
10. Nag A, V S, Bandyopadhyay S. A uniform geometric-algebraic framework for the forward kinematic analysis of 6-6 Stewart platform manipulators of various architectures and other related 6-6 spatial manipulators. Mechanism and Machine Theory 2021; 155:104090. https://doi.org/10.1016/j.mechmachtheory.2020.104090.
11. Ding X, Isaksson M. Quantitative analysis of decoupling and spatial isotropy of a generalised rotation-symmetric 6-DOF Stewart platform. Mechanism and Machine Theory 2023; 180: 105156. https://doi.org/10.1016/j.mechmachtheory.2022.105156.
12. Graba M, Bieniek A, Prażnowski K, Hennek K, Mamala J, Burdzik R, Śmieja M. Analysis of energy efficiency and dynamics during car acceleration. Eksploatacja i Niezawodność – Maintenance and Reliability 2023;25(1):17. https://doi.org/10.17531/ein.2023.1.17.
13. Wang M, Hu Y, Sun Y, Ding J, Pu H, Yuan S, Zhao J, Peng Y, Xie S, Luo J. An adjustable low-frequency vibration isolation stewart platform based on electromagnetic negative stiffness. International Journal of Mechanical Sciences 2020; 181: 105714. https://doi.org/10.1016/j.ijmecsci.2020.105714.
14. Piovesan D, Ji X. Assessment of whole-body vibration via integrating a Stewart platform and SimWise simulation. IFAC-PapersOnLine 2022; 55(37): 388–393. https://doi.org/10.1016/j.ifacol.2022.11.214.
15. Fu L, Liu Z, Cai C, Tao M, Yang M, Huang H. Joint space-based optimal measurement configuration determination method for Stewart platform kinematics calibration. Measurement 2023; 211: 112646. https://doi.org/10.1016/j.measurement.2023.112646.
16. Brouillard A. The perfect corner: a driver's step-by-step guide to finding their own optimal line through the physics of racing: 1. Paradigm Shift Motorsport Books 2016.
17. Egorov IN, Shevtsov DS. Structure of system position–force control of the drive Stewart platform. Procedia Comput Sci 2017;103:517–21. https://doi.org/10.1016/j.procs.2017.01.042.

MSc. Eng., **Jakub TYTUŁA**, student of mechatronics with research interests in mechanical engineering, diagnosis. Currently working on racing simulation peripherals with main interests focusing on motion platforms. He is currently a PhD student at the University of Warmia and Mazury in Olsztyn.
e-mail: jakub.tytula@uwm.edu.pl

MSc. Eng., **Arnold ZAREMBA**, student of mechatronics with research interests in biomedical engineering, currently working on Virtual Reality applications, focusing on mapping natural motion physics. He is currently a PhD student at the University of Warmia and Mazury in Olsztyn.
e-mail: arnold.zaremba@uwm.edu.pl

DSc. PhD. **Szymon NITKIEWICZ**, Assistant Professor in the Department of Mechatronics, Specialist in the School of Medicine, Collegium Medicum, University of Warmia and Mazury in Olsztyn. His work focuses on rehabilitation, biomechanics, biomedical engineering and diagnostics devices.
e-mail: szymon.nitkiewicz@uwm.edu.pl